

## Differences in Accuracies and Fitting Surface Planes of Two Error Models for NRTK in GPSnet

Suqin Wu, Kefei Zhang, David Silcock

School of Mathematics and Geospatial Science, RMIT University, Australia

### Abstract

In the past years, several regional error models for the network RTK (NRTK) approach have been proposed, investigated and used. Most of the studies are based on one single model to test the model's performance in a reference network or a few reference networks. Very limited research has been conducted to evaluate performance differences of different error models in the same network using the same test dataset. It is difficult to predict which of the models will outperform the others for a specific network since different reference networks have different error characteristics. For example, the multipath effect (or the station specific error), the spatial atmospheric pattern, and the scale of the ionospheric disturbance may be different in different networks. These factors may cause differences in performance among different error models.

Among the existing error models for NRTK, the linear interpolation model (LIM) and the low-order surface model (LSM) are typical and most often discussed/used. In this paper, the difference in the accuracies of the interpolated residuals in GPSnet from the two models are compared using several test cases with three different observation sessions combined with various network configurations. The snapshots of the fitting surface planes derived from the two models at the same epochs are also compared as well. Test results indicate that the LSM in some cases performed significantly poorer than the LIM. In this case, the snapshots of the two fitting surface planes from the two models present the error's correlation trend significantly different.

**Keywords:** NRTK, GPSnet, error models, regional atmospheric modelling, interpolation method

### 1. Introduction

Due to the characteristics of the spatial and temporal variation of the atmosphere, in the NRTK application, it is ubiquitous to use regional error models (or interpolation methods) for obtaining the predicted error values for the rover's location. Several regional error models proposed by different researchers in the past years for NRTK positioning mainly include:

- 1) Linear Interpolation Method (LIM) (Wanninger, 1995; Wübbena *et al.*, 1996),
- 2) Linear Combination Method (LCM) (Han, 1997; Rizos *et al.*, 1999),
- 3) Distance-based Linear Interpolation Method (DIM) (Gao *et al.*, 1997),
- 4) Low-order Surface Model (LSM) (Fotopoulos G., 2000; Fotopoulos and Cannon, 2001; Varner, 2000; Wübbena *et al.*, 1996), and
- 5) Least Squares Collocation Method (LSCM) (Raquet, 1998).

All of the error models are merely different forms of approximation for the true spatial distribution of the error modeled. Dai (2002) conducted tests for performance comparisons of all the above five models. Based on the results of a two test scenario, he concluded that all the five error models perform similarly. However, it is difficult to know if this conclusion still holds for other regions/networks. In order to investigate this, in this paper, two of these models, i.e. the LIM and the LSM are selected for the performance testing for the Victoria region using GPSnet data. The reason for this selection is that these two models both are functional models and they have more similarity in their mathematical forms, compared to other models. Secondly, both of them can be easily implemented in the data processing for real-time scenario. Moreover, these two models were commonly used ones for NRTK.

GPSnet is a regional GPS Continually Operating Reference Station Network (CORS) in the state of Victoria, Australia. Currently it consists of 33 reference stations covering both the Melbourne metropolitan and rural areas of Victoria. The inter-station distances of

GPSnet range from several tens of kilometres up to 200km, a typical medium-to-long-range GPS reference network. With the NRTK technique, GPSnet makes it possible for the high accuracy real-time positioning service to be available throughout the whole state area. The implementation and performance of the NRTK approach are currently under investigating and testing. Due to the fact that the accuracy of regional atmospheric error models is critical for the accuracy of the NRTK positioning, it is important that the performance of the error models in Victoria is assessed using the GPSnet data. Thus the performance of the NRTK in GPSnet will be enhanced, if possible (Zhang *et al.*, 2006). In order to assess the performance of regional error models in the Victoria region, tests based on both many different observation datasets and various different network configurations are more convincing. In this paper, nine test cases derived from not only three different sessions of GPSnet observations but also from a variety of four-station and five-station network configurations of sub-GPSnet are used for the performance assessment of the two selected error models.

The outline of this paper is as follows. The algorithms for the two selected error models are introduced. Secondly, the test data and the test methodology are described. Thirdly, the test results are presented. Conclusions are given in the final session.

## 2 Algorithms for the two Selected Error Models

The pre-requisite for the regional error modeling of a reference network is that ambiguities between the master station and the secondary reference stations must be first successfully resolved. Then, all of the spatially correlated errors need to be modeled to generate corrections for the rover. Ambiguity resolution for real-time medium-to-long baselines (e.g. over 100km) is very challenging. The ability to fast resolve network ambiguities and the quality of the resolved ambiguity are the two most important factors for the accuracy and quality of the correction generated and hence network RTK positioning. Procedures and algorithms for real-time network ambiguity resolutions used in this research are investigated in (Chen *et al.*, 2000) and (Wu, 2009; Wu *et al.*, 2007). In the following sections, it is assumed that all of the ambiguities between the master reference station and the secondary reference stations have been successfully fixed to their corrected values.

It should be noted that the difference between the phrases “error model” and “interpolation method” is not differentiated in this paper. This is because the only reason for the error modeling here is for obtaining the interpolated error for the rover. In this context, the two phrases being treated the same will not cause confusion.

It should also be noted that, the regional error models are designed mainly for modeling the spatially correlated errors. The spatially correlated errors consist of the orbital error and the atmospheric errors. In this research, the IGS ultra-rapid predicted orbit is used and the double-differenced (DD) approach is adopted. In this case, the residual DD orbital errors are neglectable and thus all the remained errors, which can be called combined errors, to be modelled mainly contain the DD atmospheric errors. Therefore, the *error modeling* virtually means the *atmospheric error modeling*.

In addition, the following algorithms of the two selected error models (and also other models) can be used for modeling any single types of the spatially correlated errors. They can also be used for modeling the combined errors under the assumption that each of the spatially correlated errors in the combined errors follows the same pattern of spatial correlation. In this research, the combined errors (or the atmospheric errors) are modelled.

### 2.1 Algorithms for the LIM

The initial development and use of this type of model can be found from Wanninger (1995), Wübbena *et al.* (1996), and Wanninger (1999). Chen *et al.* (2000) and Rizos *et al.* (1999) proposed to use the LIM to interpolate the combined error. The algorithm of the LIM is as follows.

The DD residual vector  $v$  (for the frequencies of either  $L_1$  or  $L_2$ ) can be defined as:

$$v = \begin{bmatrix} V_{12} \\ V_{13} \\ \vdots \\ V_{1n} \end{bmatrix} = \begin{bmatrix} \lambda \nabla \Delta \phi_{12} - \nabla \Delta \rho_{12} - \lambda \nabla \Delta N_{12} \\ \lambda \nabla \Delta \phi_{13} - \nabla \Delta \rho_{13} - \lambda \nabla \Delta N_{13} \\ \vdots \\ \lambda \nabla \Delta \phi_{1n} - \nabla \Delta \rho_{1n} - \lambda \nabla \Delta N_{1n} \end{bmatrix} = \begin{bmatrix} \Delta X_{12} & \Delta Y_{12} \\ \Delta X_{13} & \Delta Y_{13} \\ \vdots & \vdots \\ \Delta X_{1n} & \Delta Y_{1n} \end{bmatrix} \begin{bmatrix} a \\ b \end{bmatrix} \quad (1)$$

where

subscript 1 denotes the master station; 2, 3, ... $n$  denote the secondary reference stations;  $\nabla_X$  and  $\nabla_Y$  are the coordinate differences between a secondary reference station and the master station;  $a$  and  $b$  are the error model's coefficients in the directions of  $\nabla_X$  and  $\nabla_Y$  respectively. If the total number of the reference stations is more than three, the error model's coefficients  $a$  and  $b$  can be estimated by the least squares adjustment:

$$\begin{bmatrix} \hat{a} \\ \hat{b} \end{bmatrix} = (A^T A)^{-1} A^T v \quad (2)$$

where

$$A = \begin{bmatrix} \Delta X_{12} & \Delta Y_{12} \\ \Delta X_{13} & \Delta Y_{13} \\ \vdots & \vdots \\ \Delta X_{1n} & \Delta Y_{1n} \end{bmatrix} \quad (3)$$

and

$$V = \begin{bmatrix} \lambda \nabla \Delta \phi_{12} - \nabla \Delta \rho_{12} - \lambda \nabla \Delta N_{12} \\ \lambda \nabla \Delta \phi_{13} - \nabla \Delta \rho_{13} - \lambda \nabla \Delta N_{13} \\ \vdots \\ \lambda \nabla \Delta \phi_{1n} - \nabla \Delta \rho_{1n} - \lambda \nabla \Delta N_{1n} \end{bmatrix} \quad (4)$$

After  $\hat{a}$  and  $\hat{b}$  are estimated, the DD combined error for the user's location can be interpolated by

$$V_{1u} = \hat{a} \cdot \Delta X_{1u} + \hat{b} \cdot \Delta Y_{1u} \quad (5)$$

where subscript  $u$  denotes the rover user's station.

It should be noted that  $\nabla X$  and  $\nabla Y$  in equations (1) to (5) can also be replaced with  $\nabla B$  and  $\nabla L$ , which are the coordinate difference in geodetic latitude and longitude respectively at two stations. The LIM is a two dimensional (2D) model as only two variables ( $\nabla X$  and  $\nabla Y$ ) are used in the model.

## 2.2 Algorithms for the LSM

The low-order surface models usually refer to the first-order and the second-order surface models. These models can also be used to fit the distance-dependent error (Fotopoulos G., 2000; Wübbena *et al.*, 1996). The fitted surface shows the major trend of the distance-dependent error. The number of variables in the regression function is two when plane coordinates  $X$  and  $Y$  (or  $B$  and  $L$ , latitude and longitude) are used as variables. The fitting surface plane is two dimensional. In the case where  $X$ ,  $Y$  and  $H$  (height component) are used as variables, a three dimensional surface model is used. In practice, the correlation nature of the error in each of the three directions is the determining factor for choosing a suitable model. In the application of the GPS error modeling, special care should be taken to see the necessity of the inclusion of the vertical component  $H$  in the model. The reason is that, in many cases, it is not meaningful to use it, e.g. when the height difference among the reference stations is very small, or, when the error to be modeled doesn't exhibit the spatially-correlated nature in the vertical direction. In these two cases, the inclusion of  $H$  in the model needs more coefficients to be resolved. Consequently more reference stations are required. This is a key disadvantage of using more variables or/and a higher order surface model.

The height difference ( $H$ ) among the reference stations of GPSnet is under 0.5km. Neglecting such amount of  $H$  in the error model will affect the performance of the model little. According to Fotopoulos (2000) and Schaer (1999), the difference between two-dimensional and three-dimensional models is small even for a regional network with more than 3000 metres of inter-station height differences.

The two dimensional model used in this research is the typical first-order surface model. The formula of this

model can be expressed as (Dai *et al.*, 2004; Fotopoulos G., 2000):

$$V = a \cdot \Delta X + b \cdot \Delta Y + c \quad (6)$$

where  $V$  is the DD residual that can be calculated from equation (4);  $\Delta X$  and  $\Delta Y$  are the horizontal coordinate differences between the secondary stations and the master station;  $a$ ,  $b$  and  $c$  are the model's coefficients. The model's coefficients can be estimated by the least squares adjustment if there are redundant reference stations.

The least square estimates for the coefficients in equation (6) can be obtained:

$$\begin{bmatrix} \hat{a} \\ \hat{b} \\ \hat{c} \end{bmatrix} = (A^T A)^{-1} A^T V \quad (7)$$

where

$$A = \begin{bmatrix} \Delta X_{12} & \Delta Y_{12} & 1 \\ \Delta X_{13} & \Delta Y_{13} & 1 \\ \vdots & \vdots & \vdots \\ \Delta X_{1n} & \Delta Y_{1n} & 1 \end{bmatrix} \quad (8)$$

In a similar way that equation (5) is used for the LIM, then the DD interpolated corrections for the rover can be calculated by:

$$V_{1u} = \hat{a} \cdot \Delta X_{1u} + \hat{b} \cdot \Delta Y_{1u} + \hat{c} \quad (9)$$

The minimum number of reference stations required for the first-order 2D surface model expressed in equation (6) is four as the DD approach is used. One more reference station is required for the extra constant term  $c$ , compared to the LIM.

From the 2D LIM and the first-order 2D LSM, it can be seen that the only difference in the two fitting functions is the constant term  $c$  that presents in the LSM. For the same test dataset, the coefficients  $\hat{a}$  and  $\hat{b}$  derived from the two models do not necessarily have the same values. This is especially true when multipath effects exist at some (or all) of the reference stations. The term  $c$  in the LSM was not designed for modeling the spatially correlated error like  $\hat{a}$  and  $\hat{b}$  do, instead, it was for modeling the station specific errors of the master station. It may make sense for the undifferencing approach. However in the DD approach, it is in fact for modeling the station specific errors of the network. This means that the constant term represents the averaged value of the station specific errors of all the stations. The residual station specific errors of all the stations will be absorbed in  $\hat{a}$  and  $\hat{b}$ .

In the LIM, all station specific errors are not explicitly modeled in the way that the LSM does, they will all be

absorbed in its  $\hat{a}$  and  $\hat{b}$ . Theoretically, it is difficult to determine whether the LIM or the LSM outperforms the other, especially when station specific errors exist in the network. For a specific network, the differences in the interpolation accuracy of the two models may reflect which model can mitigate the station specific errors more efficiently than the other. This is also one of the main purposes of the tests conducted in this research.

### 3 Test Data and Network Configurations

The test data used for this research is from selected GPSnet sites. The names and network configurations of the six selected reference stations are shown in Fig. 1 and Fig.2. Park station is located inside the polygon formed by all of the other reference stations. Therefore, it is selected as the rover station for the purpose of checking and validating the test results. The GPS data from three different observation sessions is selected for the tests. The three time sessions are defined as Time1 (3:50pm-9:30pm on 13/11/2007), Time2 (8:20am-11:00am on 26/07/2008) and Time3 (1:30pm-4:00pm on 1/06/2007) respectively. All the times are the local time. In each session, there are several different network configurations that are for various test cases. For convenience, Group1, Group2 and Group3 are labeled to represent all of the tests in each of the three sessions respectively. For example, Group1 is for all of the test cases of the first session (i.e. Time1), Group2 is for all of the test cases of the second session (i.e. Time2) and Group3 is for all of the test cases of the third session (i.e. Time3).

As shown in Figs. 1 and 2, the selected baselines (in red) for the tests of Group1 and Group2 are Bacc-Park and Morn-Park respectively. The baseline lengths and positions of all the reference stations can be seen in Figs. 1 and 2 as well. For Group3, the test baseline and the fundamental network configurations are the same as that of Group2 however the observation session is different (i.e. Time3). The sampling rates of the data from the three sessions are 30 seconds, 5 seconds and 10 seconds respectively.

From Figs. 1 and 2, one can see that the lengths of the two test baselines are: 47.7km for Bacc-Park and 48.6km for Morn-Park. The network is a typical mid-range-baseline network in the context of NRTK as all baselines from the secondary reference stations to the master station are in the range of 53-97km.

Tables 1, 2 and 3 list the network configurations that will be used in the next section for the tests of Group1, Group2 and Group3 respectively. Each of the three tables contains the five-station configurations and two four-station configurations (since the minimum number of reference stations required for the LSM is four).

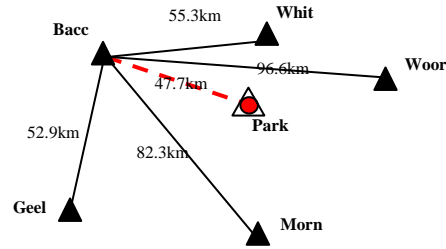


Fig. 1 Test baseline for Group1 and network from GPSnet

Table 1 Network configurations for the tests of Group1 (i.e. observations from Time1)

Configuration	Stations selected
Cfg.1	All of the five stations
Cfg.2	Bacc, Morn, Woor, Whit
Cfg.3	Bacc, Morn, Geel, Woor

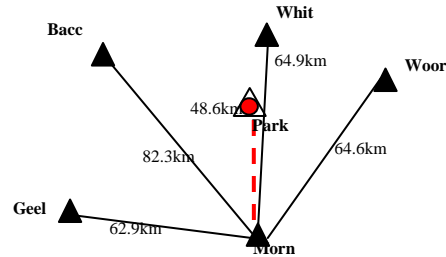


Fig. 2 Test baseline for Group2 and Group3 from GPSnet

Table 2 Network configurations for the tests of Group2 (i.e. observations from Time2)

Configuration	Stations included
Cfg.1	All of the five stations
Cfg.2	Morn, Geel, Bacc, Whit
Cfg.3	Morn, Geel, Bacc, Woor

Table 3 Network configurations for the tests of Group3 (i.e. observations from Time3)

Configuration	Stations included
Cfg.1	All of the five stations
Cfg.2	Morn, Geel, Whit, Woor
Cfg.3	Morn, Bacc, Whit, Woor

It should be noted that all the tests are conducted in a post-processing mode but the approach is for real-time since the algorithms used in the data processing is on an epoch-by-epoch, a station-by-station and a satellite-by-satellite basis.

## 4 Test Results

### 4.1 Interpolation Accuracies

#### 4.1.1 Results for Group1

The network configurations for this group’s testing are from Table 1 and the satellite selected is PRN13. The time series plots for the original/measured DD L1 residuals and the residuals with corrections from the two models are shown in Figs. 3a, 3b and 3c.

Figs 3a and 3b show that the accuracies of the LIM’s results (in red) are significantly better than that of the LSM since the former are more close to zero, whereas Fig. 3c shows the similar accuracies of the two models for its configuration. These three figures also show that all of the LIM results are significantly improved, compared to the original residuals. However the LIM’s results are significantly different: in some configurations (i.e. Figs. 3a and 3c) and at some epochs (Fig. 3b), its results are significantly improved, while at other epochs its results are even worse than the original residuals (i.e. the later part of Fig. 3b).

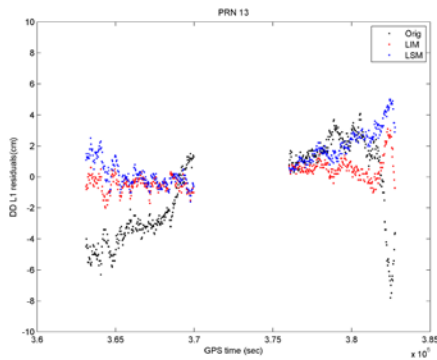


Fig. 3a Time series plots for the original/measured DD L1 residuals and the residuals with corrections from the LIM and LSM respectively, for baseline Bacc-Morn in Cfg.1 of Table 1

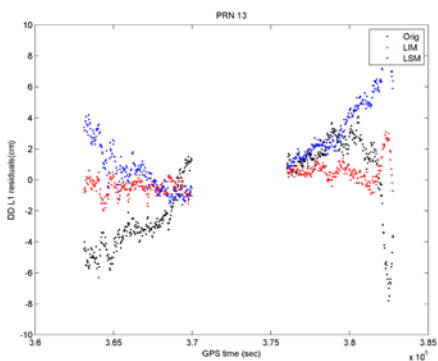


Fig. 3b Time series plots for the original/measured DD L1 residuals and the residuals with corrections from the LIM and LSM respectively, for baseline Bacc-Morn in Cfg.2 of Table 1

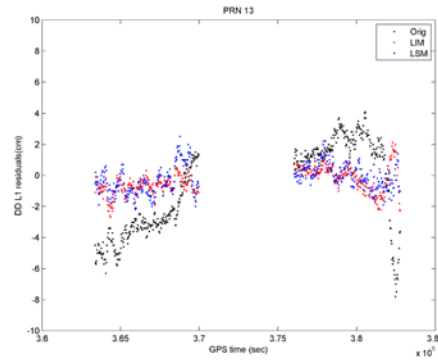


Fig. 3c Time series plots for the original/measured DD L1 residuals and the residuals with corrections from the LIM and LSM respectively, for baseline Bacc-Morn in Cfg.2 of Table 1

It should be noted that in these three figures, the middle part of the plots are blank. This is because PRN13 is selected as the reference satellite for the DD during that period of time. The NRTK system automatically selects the satellite that has the highest elevation angle at an epoch to be the reference satellite for the epoch. In addition, for the DD results, instead of quote a pair of satellites, only one satellite (i.e. PRN13) is mentioned here. The reason for that is the varying reference satellite for different epochs in the time series. Usually several satellites are used as the reference satellite for the time series.

#### 4.1.2 Results for Group2

The network configurations for this group’s testing are from Table 2 and the satellite selected is PRN29. The time series plots for this group’s testing are shown in Figs. 4a, 4b and 4c.

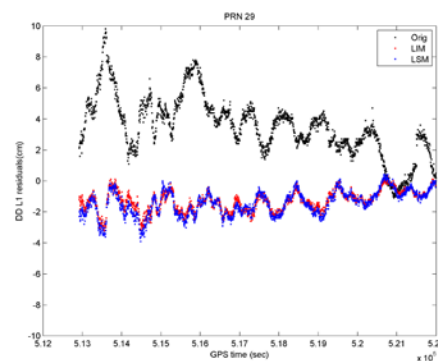


Fig. 4a Time series plots for the original/measured DD L1 residuals and the residuals with corrections from the LIM and LSM respectively, for baseline Morn-Bacc in Cfg.1 of Table 2

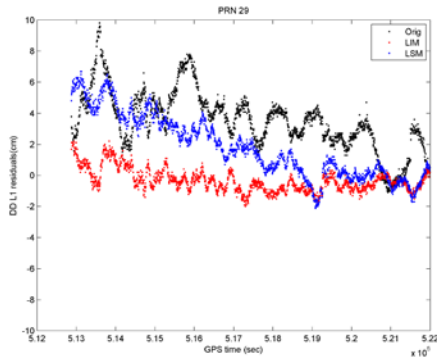


Fig. 4b Time series plots for the original/measured DD L1 residuals and the residuals with corrections from the LIM and LSM respectively, for baseline Morn-Bacc in Cfg.2 of Table 2

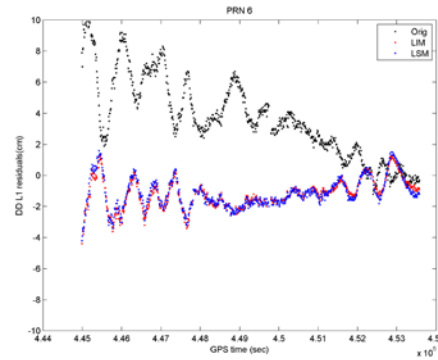


Fig. 5a Time series plots for the original/measured DD L1 residuals and the residuals with corrections from the LIM and LSM respectively, for baseline Morn-Bacc in Cfg.1 of Table 3

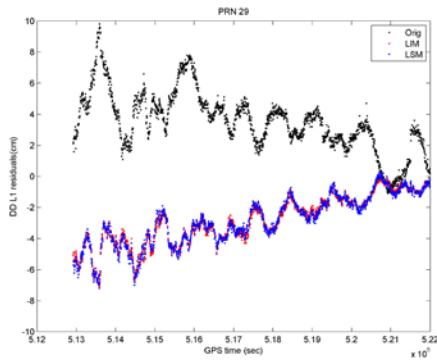


Fig. 4c Time series plots for the original/measured DD L1 residuals and the residuals with corrections from the LIM and LSM respectively, for baseline Morn-Bacc in Cfg.3 of Table 2

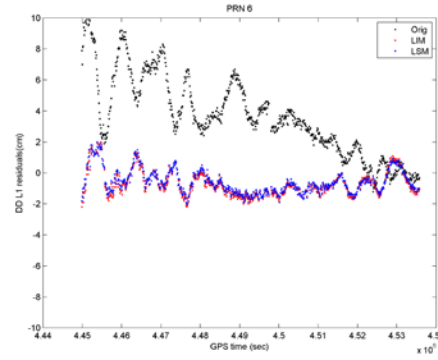


Fig. 5b Time series plots for the original/measured DD L1 residuals and the residuals with corrections from the LIM and LSM respectively, for baseline Morn-Bacc in Cfg.2 of Table 3

These three figures also show that all of the DD residuals with the two models' corrections can be significantly improved, compared to the original DD residuals. Figs 4a and 4c shows no significant difference in the accuracies of the interpolated results between the LIM and LSM, whereas Fig. 4b shows that the LIM's results are significantly better than that of the LSM.

### 4.1.3 Results for Group3

The network configurations for this group's testing are from Table 3 and the satellite selected is PRN6. The test results are shown in Figs. 5a, 5b and 5c.

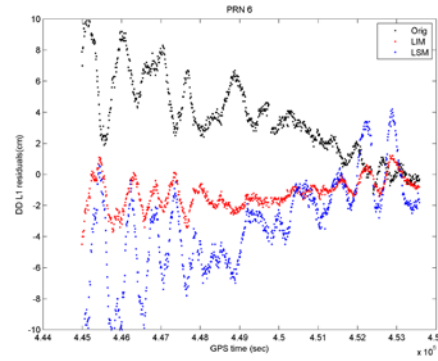


Fig. 5c Time series plots for the original/measured DD L1 residuals and the residuals with corrections from the LIM and LSM respectively, for baseline Morn-Bacc in Cfg.3 of Table 3

Figs. 5a and 5b show the similarity of the interpolation accuracies between the two models. However Fig. 5c shows that the DD residuals with the LIM's corrections are all significantly improved, compared to the original residuals, whereas the residuals with the LSM's corrections at some epochs are even worse than the original residuals.

## 4.2 Fitting Surface Planes

The aforementioned test results are from the final interpolated results derived from the two error models. These interpolated results are calculated from equations (5) and (9) that virtually represent the 2D fitting surface planes derived from the two models. In this section, the snapshots of the 2D fitting surface planes from the two models at some epochs are created since they graphically represent the error variation trend at the epoch. From the comparisons of the error variation trends represented by the two models' coefficients for the same epochs, the relationship between the trend difference and the performance difference of these two error models at each of the epochs can be investigated.

### 4.2.1 Snapshots for an epoch in Group1

Figs. 6a, 6b and 6c are the three sets of fitting surface planes at the GPS time (epoch) of 382620 second. The three network configurations, the test baseline and the satellite selected (i.e. PRN13) selected for the error modelling are the same as that of section 4.1.1. The two sets of parallel lines at the bottom part of each figure are the 2D contour lines.

From both fitting planes and contour lines, the spatial variation trend and the variation rate (or gradient) of the DD residuals in any directions can be seen. The greatest gradient is along the intersected line of the fitting plane and the perpendicular plane to the set of contour lines that are for the fitting plane. The trend difference of two fitting planes can be measured by some of the plane's features e.g. the spatial ascending/descending directions, the direction and magnitude of the (greatest) spatial gradient etc.

Fig. 6a shows that the directions of the two sets of contour lines are similar. This means the spatial ascending/descending directions of the residuals represented by the two models are similar. However the spatial gradients of the two planes are significantly different. Fig. 6b shows significant difference in both directions of the two sets of contour lines and the spatial gradient of the residuals. Fig. 6c shows no significant differences in both the ascending direction and the spatial gradient are s the represented by the two planes. Thus, the difference in the accuracy of the final interpolated residuals between the two models in Fig. 6c ( $1.4\text{cm}-0.5\text{cm}=0.9\text{cm}$ ) is much less than that of Fig. 6a and Fig. 6b ( $3.1\text{cm}$  and  $5.8\text{cm}$ ).

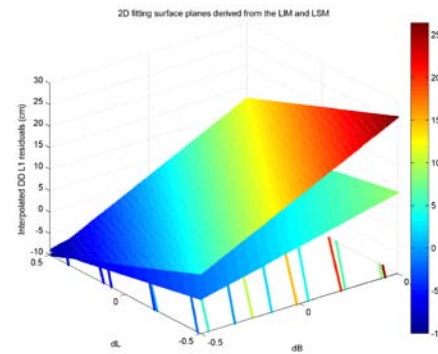


Fig. 6a for Cfg.1 of Table 1 (5 stns). The accuracies of the interpolated residuals from the LIM and LSM are 1.8cm and 4.9cm respectively

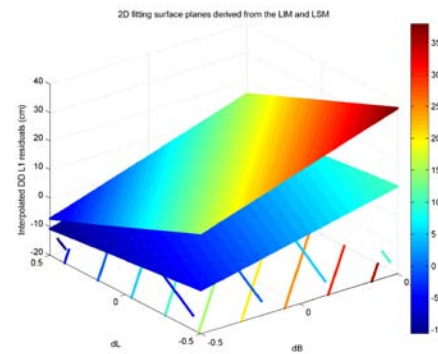


Fig. 6b for Cfg.2 of Table 1 (4 stns). The accuracies of the interpolated residuals from the LIM and LSM are 1.8cm and 7.6cm respectively

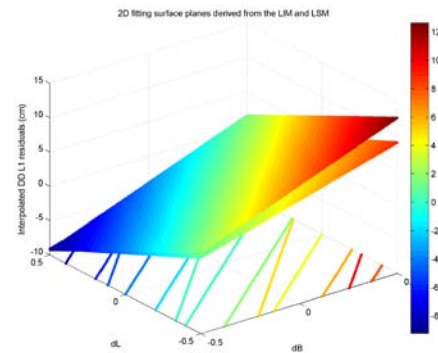


Fig. 6c for Cfg.3 of Table 1 (4 stns). The accuracies of the interpolated residuals from the LIM and LSM are 0.5cm and 1.4cm respectively

### 4.2.2 Snapshots for an epoch in Group2

Figs. 7a, 7b and 7c are the three sets of fitting surface planes at the GPS time (epoch) of 513600 second. The three network configurations, the test baseline and the satellite selected (i.e. PRN29) selected for the error modelling are the same as that of section 4.1.2.

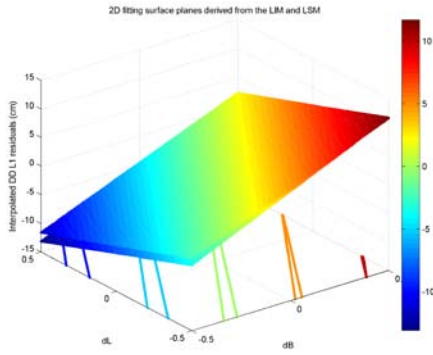


Fig. 7a for Cfg.1 of Table 2 (5 stns). The accuracies of the interpolated residuals from the LIM and LSM are -2.6cm and -2.8cm respectively

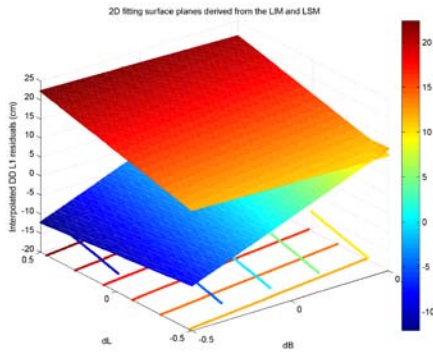


Fig. 7b for Cfg.2 of Table 2 (4 stns). The accuracies of the interpolated residuals from the LIM and LSM are -0.5cm and 5.2cm respectively

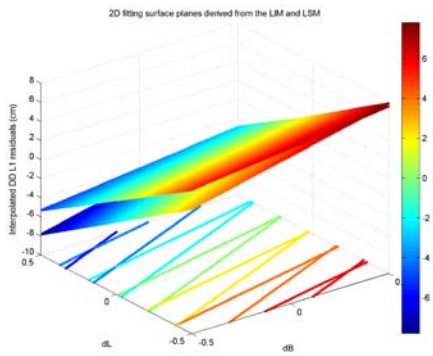


Fig. 7c for Cfg.3 of Table 2 (4 stns). The accuracies of the interpolated residuals from the LIM and LSM are -6.4cm and -6.3cm respectively

Fig. 7b shows that both the directions of the spatial ascending and the overall colours (meaning the residual values) of the two planes are significantly different. These lead to the significant difference (5.2cm-(-0.5cm)=5.7cm) in the accuracies of the interpolated residuals from the two models. However Fig. 7a and 7c are different. The similarity in the two planes in each of the two figures leads to the similar interpolation accuracies.

### 4.2.3 Snapshots for an epoch in Group3

Figs. 8a, 8b and 8c are the three sets of fitting surface planes at the GPS time (epoch) of 446360 second. The three network configurations, the test baseline and the satellite selected (i.e. PRN6) selected for the error modelling are the same as that of section 4.1.3.

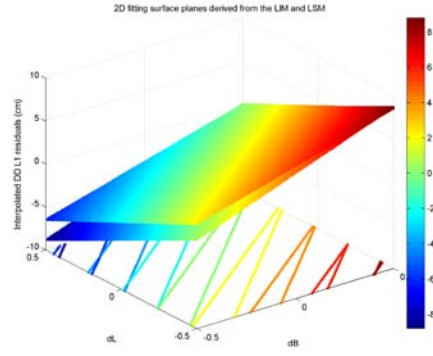


Fig. 8a for Cfg.1 of Table 3 (5 stns). The accuracies of the interpolated residuals from the LIM and LSM are -0.2cm and 0.0cm respectively

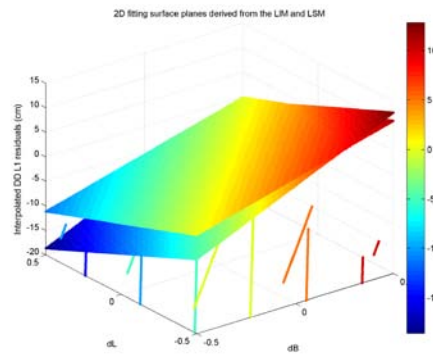


Fig. 8b for Cfg.2 of Table 3 (4 stns). The accuracies of the interpolated residuals from the LIM and LSM are 1.1cm and 1.2cm respectively

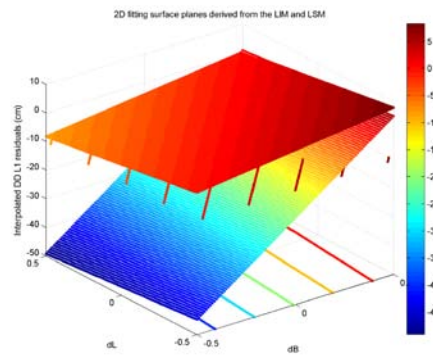


Fig. 8c for Cfg.3 of Table 3 (4 stns). The accuracies of the interpolated residuals from the LIM and LSM are -0.3cm and -4.8cm respectively

Likes Fig. 7b, Fig. 8c also shows the significant difference in both the spatial gradients and the colour ranges between the two planes, which lead to the

significant difference in the accuracies of the interpolated results from the two models (5.1cm). Figs .8a and 8b also show the results similar to that of Figs. 7a and 7c.

## 5. Conclusions

In this paper, comparisons for accuracies of the interpolated residuals derived from the two selected error models for NRTK: the LIM and the LSM, for three time series are conducted. Comparisons for the snapshots of the 2D fitting surface planes from the two models at three epochs are also presented. The test samples contain three difference sessions of observations, combined with various network configurations including five reference stations and four reference stations from the GPSnet sites. The test results show that the accuracy of the DD residuals with the LIM's corrections can be always significantly improved. However residuals with the corrections of the LSM sometimes can be much worse than the residuals without the corrections. The test results also shows that when the 2D fitting surface planes derived from the two error models' coefficients at the same epoch show significant difference in the spatial variation trend, the two models' accuracies are also significantly different. On the other hand, when both the spatial ascending/descending directions and the spatial gradients the two planes presented have no significant differences, the accuracies of the interpolated residuals from the two error models are similar.

Based on the fact that when the LSM performs very poorly, the accuracy of the interpolated residual from the LIM is however very high and much higher than that of the LSM, it can be assumed that the LIM's fitting surface plane is much closer to the real trend of the error's spatially correlation than the LSM's. In this case, the LSM's fitting plane is assumed to be more distorted, compared to the LIM's. It should be pointed out that this assumption is only based on the accuracy of one rover point's interpolation results in GPSnet. It may not be conclusive to say that the LIM's fitting plane has a smaller discrepancy with the real spatial trend of the error because of its better interpolation accuracy. However, the focus has been mainly on the comparison of differences between the two fitting planes of the two models rather than the differences between either of them and the real error plane.

## Acknowledgments

The author would like to gratefully acknowledge the research funds granted for this project through the Australian Research Council (LP0455170).

## References

- Chen, X., Han, S., Rizos, C. and Goh, P. C. (2000) *Improving real-time positioning efficiency using the Singapore Integrated Multiple Reference Station Network (SIMRSN)*. 13th Int. Tech. Meeting of the Satellite Division of the U.S. Inst. of Navigation, Salt Lake City, Utah, USA, Sept. 19–22, 9–18.
- Dai, L., Han, S., Wang, J. and Rizos, C. (2004) *Comparison of Interpolation Algorithms in Network-Based GPS Techniques*. Navigation, 50(4): 277–293.
- Dai, L. W. (2002) *Augmentation of GPS with GLONASS and pseudolite signals for carrier phase-based kinematic positioning*. Ph.D Thesis, School of Surveying & Spatial Information Systems, The University of New South Wales, Sydney, Australia.
- Fotopoulos, G. (2000) *Parameterization of Carrier Phase Corrections Based on a Regional Network of Reference Stations*. ION GPS-2000, Salt Lake City, Utah, USA, Sept.19–22, 1093–1102.
- Fotopoulos, G. (2000) *Parameterization of DGPS Carrier Phase Errors Over a Regional Network of Reference Stations*. Master Thesis, Department of Geomatics Engineering, University of Calgary, Calgary, Canada.
- Fotopoulos, G. and Cannon, M. E. (2001) *An Overview of Multi-Reference Station Methods for cm-Level Positioning*. GPS Solutions, 4(3): 1–10.
- Gao, Y., Li, Z. and McLellan, J. F. (1997) *Carrier phase based regional area differential GPS for decimeter-level positioning and navigation*. 10th Int. Tech. Meeting of the Satellite Div. of the U.S. Institute of Navigation, Kansas City, Missouri, USA, Sept. 16–19, 1305–1313.
- Han, S. W. (1997) *Carrier Phase-Based Long-Range GPS Kinematic Positioning*. Ph.D Thesis, School of Geomatic Engineering, The University of New South Wales, Sydney, Australia.
- Raquet, J. F. (1998) *Development of a Method for Kinematic GPS Carrier-Phase Ambiguity Resolution Using Multiple Reference Receivers*. Ph.D Thesis, Department of Geomatics Engineering, University of Calgary, Calgary, Canada.
- Rizos, C., Han, S. and Chen, H. Y. (1999) *Regional-Scale Multiple Reference Stations for Real-time Carrier Phase-Based GPS Positioning: A Correction Generation Algorithm*. Int. Symp. on GPS: Application to Earth Sciences & Interaction with Other Space Geodetic Techniques, Tsukuba, Japan, Oct. 18–22.
- Schaer, S. (1999) *Mapping and Predicting the Earth's Ionosphere Using the Global Positioning System*. Ph.D Thesis, University of Berne, Berne, Switzerland.
- Varner, C. (2000) *DGPS carrier phase networks and partial derivative algorithms*. Ph.D Thesis, Dept. of Geomatics Engineering, University of Calgary, Calgary, Canada.
- Wanninger, L. (1995) *Improved Ambiguity Resolution by Regional Differential Modelling of the Ionosphere*. Proceedings of the ION GPS 95, Palm Springs, California,

USA, Sept. 12–15, 55–62.

Wanninger, L. (1999) *The performance of virtual reference stations in active geodetic GPS-networks under solar maximum conditions*. 12th Int. Tech. Meeting of Satellite Div. of the U.S. Institute of Navigation, Nashville, Tennessee, USA, Sept. 14–17, 1419–1427.

Wu, S. (2009) *Performance of Regional Atmospheric Error Models for NRTK in GPSnet and the Implementation of A NRTK System*. PhD Thesis, School of Mathematical and Geospatial Sciences, RMIT University, Melbourne, Australia.

Wu, S., Zhang, K. and Wu, F. (2007) *Atmospheric Effect Modelling for Victoria Network RTK-A Preliminary Performance Assessment*. International Global Navigation Satellite Systems Society IGNSS Symposium 2007, Sydney, Australia, Dec. 4–6.

Wübbena, G., Bagge, A., Seeber, G., Böjer, V. and Hankemeier, P. (1996) *Reducing distance dependent errors for real-time precise DGPS applications by establishing reference station networks*. 9th Int. Tech. Meeting of the Satellite Div. of the U.S. Institute of Navigation, Kansas City, Missouri, USA, Sept. 17–20, 1845–1852.

Zhang, K., Wu, F., Wu, S., Rizos, C., Roberts, C., Ge, L., Yan, T., Gordini, C., Kealy, A., Hale, M., Ramm, P., Asmussen, H., Kinlyside, D. and Harcombe, P. (2006) *Spare or Dense: Challenges of Australian Network RTK*. Proceedings of IGNSS Conference 2006, Queensland, Australia, July 18–21.